Progress In Electromagnetics Research M, Vol. 90, 195–203, 2020

Development of Circular Loop Frequency Selective Surface Using 3-D Printing Technique

Deepika Singh*, Abhinav Jain, and Rana P. Yadav

Abstract—This paper discusses a circular loop frequency selective surface (FSS) using a 3-D (three dimensional) printing technique. The proposed FSS design consists of a metallic patch having a circular loop printed on one side of Acrylonitrile Butadiene Styrene (ABS) material. This design is used for harmonic radar applications at 5 GHz resonant frequency. Various FSS parameters are discussed to show the effect on the resonant frequency. To make fabrication process easier and cost-effective, transmitting and receiving antennas are also printed using a 3-D printing material. 3-D printing offers cost-effective fabrication technique compared with other conventional techniques and helps in rapid prototyping. The fabricated prototype is validated with the experimental results that show good agreement between simulated results and the measured ones.

1. INTRODUCTION

Frequency Selective Surfaces (FSSs) are generally constructed from the periodic array of slots of arbitrary geometry within the conducting sheet or periodic array of metallic patches on the substrate [1]. Using these geometries, FSS transmits electromagnetic waves at a specific frequency. Basically, there are two geometries that are to be discussed for FSS [2]. The first geometry or inductive FSS corresponds to a high pass filter while the second geometry or capacitive geometry corresponds to a low pass filter [2]. If periodic elements of FSS show resonance behavior, then inductive FSS will exhibit total transmission characteristics while capacitive FSS will exhibit total reflection in the neighborhood of elements resonance. The capacitance is obtained from the gaps between the adjacent conducting dipoles/slots while inductance results are due to current from dipoles or around the loop in slots [3]. FSS can be seen as an extensive area of intensive research due to its widespread applications in the field of optical and spatial microwave filters for many decades [4].

FSS has versatile functionalities, due to which, it has found applications from lower microwave to terahertz frequencies for a long time [5]. They can be used for RCS reduction [6], polarization converter [7], radar absorbing materials [8], etc. One of the main applications of FSS is wireless security. Generally, FSSs are incorporated on the walls of a building in order to provide WLAN (wireless local area network) security. These FSSs block WLAN signal while bypassing the cell phone signals [9], but they give high stopband reflection that causes delay spread in WLAN application. Recently, researches are working in stealth applications [10–12]. For stealth applications, it becomes necessary to reduce the radar cross-section (RCS) [6] of antennas. Most of these antennas act as scatters for other frequency bands that lie outside their desired frequency band. In RCS, it is desired to reduce higher order modes so that they could not interfere in stealth applications [13]. Most of the FSSs have been fabricated using the conventional Printed Circuit Board (PCB) technique that requires complex procedures. Three-dimensional (3-D) printing can be used for fabricating any planar, non-planar, complicated geometry in a single step [14, 15].

Received 14 January 2020, Accepted 25 March 2020, Scheduled 1 April 2020
* Corresponding author: Deepika Singh (deepikasingh806@gmail.com).
The authors are with the Department of ECE, Thapar Institute of Engineering & Technology, Patiala, India.

In this paper, we design an FSS for harmonic radar applications. Harmonic radar is used to study detailed analysis of known objects. In a traditional radar, it is almost impossible to detect the objects since the reflected wave contains the signal of plants, soil, etc. due to the cluttered environment. So, in a harmonic radar, tag or transponder is attached with the target element so that its location can be determined even in the cluttered environment [16]. The tag makes use of radar signal as an energy source and re-emits the second harmonic of the transmitted frequency signal. In this way, signal can be received even without on-board energy signal source. By tuning the receiver with the harmonic frequency, the signal can be identified even in the presence of background clutter. The ability of FSS to produce harmonics of transmitted signal for either bandpass or band-reject signal makes it a potential candidate for harmonic radar applications.

This paper deals with the FSS design having a square patch with circular ring slots rejecting the signal at 2.5 GHz while passing at 5 GHz frequency band. In this way, the signal rejects fundamental frequency and passes the second harmonic frequency for harmonic radar applications. Generally, circular ring is considered much better in terms of sensitivity, angular stability, bandwidth, and cross-polarization than other shaped elements. Many researchers are working on reducing the fabrication cost of PCB, which can be easily solved by using acrylonitrile butadiene styrene (ABS) 3-D printing material [17]. The geometrical complex FSS can be easily fabricated by ABS material that is cost-effective, readily available, and effective for rapid prototyping. The geometrical dimension of a unit cell is $0.42\lambda_0 \times 0.42\lambda_0$ where λ_0 is the wavelength corresponding to bandpass resonant frequency (5 GHz). The prototype has a dimension of 175 mm $\times$ 175 mm and is fabricated using 3-D printing with conducting coating paint across the metallic parts. Section 2 shows the design structure of unit cell. Section 3 elaborates the simulated results. Parametric discussion is illustrated in Section 4, and fabricated prototype procedure is presented in Section 5. Section 6 deals with experimental results, and last Section 7 briefs the work done.

2. FSS UNIT CELL CONFIGURATION

Based upon the circuit theory, the frequency filtering characteristic of an FSS can be represented by its equivalent circuit model [18]. Depending on the frequency response of FSS, FSS is characterized by an inductive or capacitive element or combination of both. When the perpendicular plane wave impinges on the surface of FSS, capacitance is created between the gaps of adjacent loops of conducting surface due to the effect of electric charge accumulation. This accumulation of electric charge densities in horizontal strips of loop lead to the formation of capacitance. On the other hand, inductance is formed around the adjacent loops due to the current flow. The magnetic field induced in vertical strips due to electric current flow forms the inductive part.

The layout of proposed FSS design is shown in Fig. 1(a). The FSS structure consists of a square patch with circular ring slots [19] backed by ABS substrate material. The ABS material with dielectric constant of 2.8 and loss tangent of 0.0051 is used for the design of the proposed FSS. p represents the periodicity of unit cell, l the length of patch, h the height of substrate, and $r1$, $r2$, and $r3$ are inner, middle, and outer loops, respectively. The optimized parameters for resonant frequency are $p = 25$ mm, $l = 24.5$ mm, $r1 = 5$ mm, $r2 = 8$ mm, and $r3 = 11$ mm, $h = 1.5$ mm. Each successive ring differs by radius of 3 mm.

In order to avoid grating lobes and scattering in undesired directions, periodicity of elements should be less than the shortest wavelength of incident angle (0°). For greater incident angle, periodicity should be equal to half free space wavelength for avoiding grating lobes. The general formula showing the condition for placing the FSS elements in a lattice is:

$$\frac{p}{\lambda} < \frac{1}{(1+\sin\theta)} \tag{1}$$

where p is the periodicity of elements, λ the wavelength, and θ the angle of incidence.

The equivalent circuit model of the proposed design is shown in Fig. 1(b). The capacitance C_1 is introduced due to the gap between unit cells. L_1 is created due to metallic patch while C_2 and L_2 appear due to slot and metallic circular rings, respectively. The impedance of proposed design is obtained as:

$$Z = \frac{\left(-\omega^2 C_1 L_2 + 1\right) L_1 + L_2\left(-w^2 L_1 C_2 + 1\right)}{j\omega L_1 C_1\left(1 - \omega^2 L_2 C_2\right) + j\omega(L_2 C_1)} \tag{2}$$

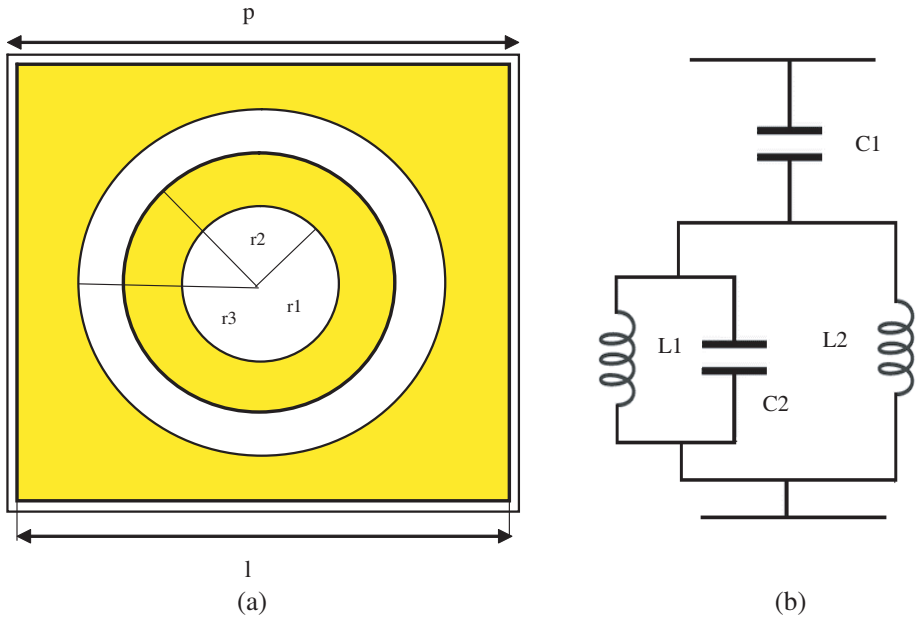

Figure 1. (a) Layout of proposed FSS. (b) Equivalent Circuit model of proposed design.

The values of poles and zeros can be easily obtained by keeping the values of numerator and denominator of above equation equal to zero. The optimized values of L_1, L_2, C_1, and C_2 are calculated to be 1.18 nH, 1.01 nH, 4.74 pF, and 1.95 pF, respectively.

3. SIMULATED RESULTS

The designed FSS is optimized and simulated in CST microwave studio using frequency domain solver. By applying the Floquet boundary condition, the FSS structure is assumed to be an infinite array of FSS unit cell. The boundary conditions are set to be unit cell boundary and have meshing set as tetrahedral meshing. Fig. 2(a) shows the comparison of various stages in design of the proposed FSS. Fig. 2(b) shows the transmission response of the proposed design having resonant bandpass frequency at 5 GHz and band reject frequency at 2.5 GHz. As seen from Fig. 2(c) and (d), at an oblique angle of incidences, resonant bandpass frequency is almost similar for both TE as well as TM mode for lower angles. As the oblique angle increases, the effect of grating lobe starts dominating for both the modes. For higher angles, dual bandpass frequency has appeared for TE mode. Another band reject frequency starts dominating at 5.2 GHz and 6.184 GHz in the case of TE mode and at 6.94 GHz in the case of TM mode at an angle of 60°. For TM mode, there is greater stability for bandpass resonant frequency at higher incidence angle while there is a frequency shift by 0.25 GHz around band reject frequency from 0° to 60°.

4. PARAMETRIC DISCUSSION

The main key parameters which affect the performance of designed FSS are radius of loops ($r1$, $r2$, $r3$), period of unit cell (p), and the gap between unit cells. The radii of loops strongly affect the resonant frequency while keeping other parameters unchanged as seen in Figs. 3(a), (b), and (c). Inner loop does not have much effect on the resonant frequency except 3-dB bandwidth which is decreased with an increase in the radius of loop ($r1$). The middle loop radius ($r2$) strongly affects the resonant frequency which is decreased with an increase in radius of loop and vice versa. As seen in Fig. 3(b), as the radius of middle loop ($r2$) increases, there is a sharp dip of 0.5 GHz frequency from 5 GHz to 4.5 GHz. On the other hand, with a decrement in the middle loop radius, there is a sharp increment of 0.5 GHz frequency.

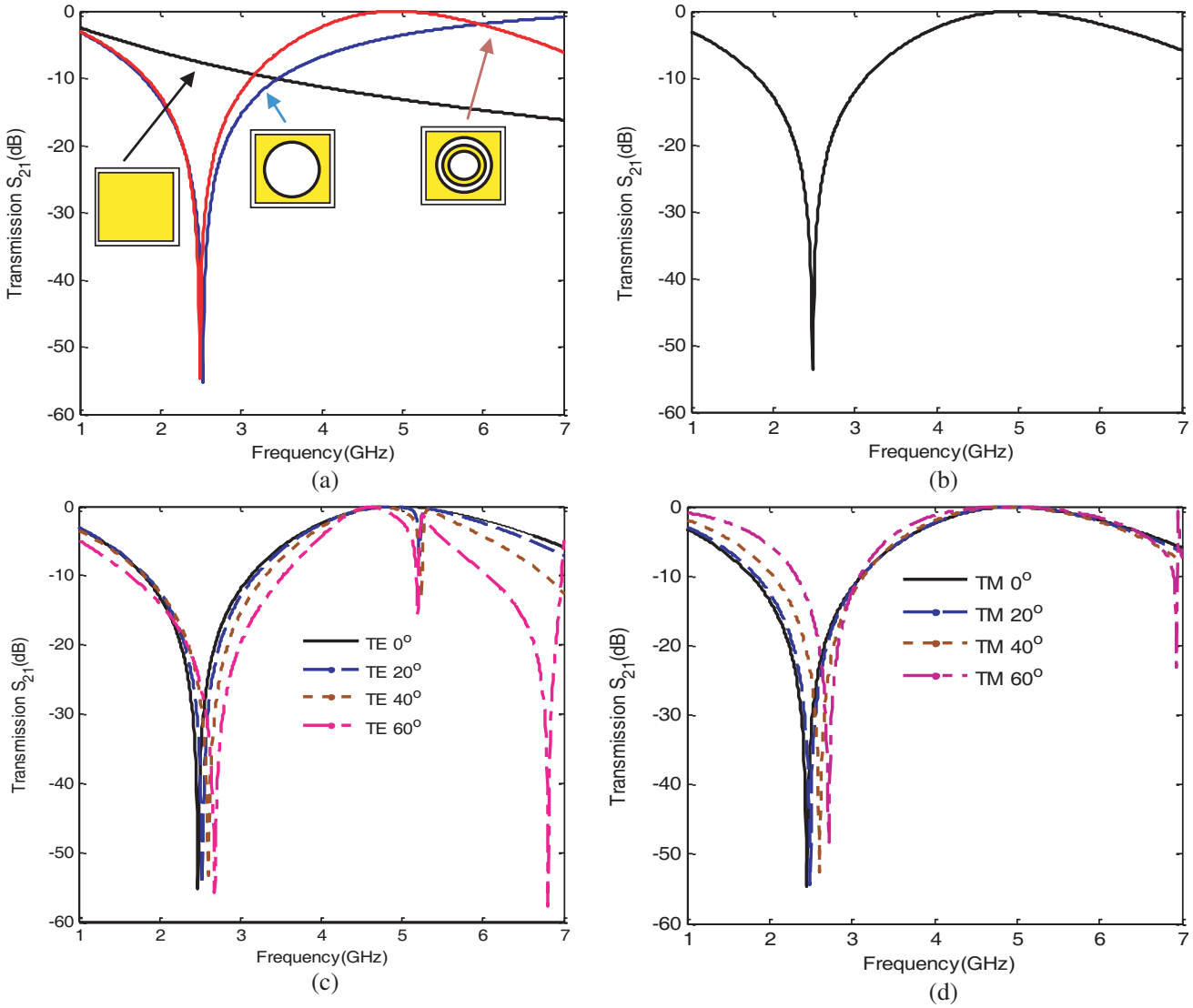

Figure 2. (a) Comparison of transmission response at various designing stages. (b) Transmission response of unit cell. (c) Effect of different incidence angles on TE mode and. (d) TM mode.

The outer loop radius ($r3$) also impacts the bandpass frequency which decreases with an increase in the radius of loop, and band reject fundamental frequency is also decreased by 0.4 GHz from 2.5 GHz to 2.1 GHz with increment in radius and vice versa. As the width of conducting loop increases, inductance of the loop will decrease and vice versa. Similarly, as the width of non-conducting loop increases, capacitance of the loop will decrease and vice versa. The inductance and capacitance greatly affect the resonant frequency of the FSS structure. Generally, the periodicity of unit cell impacts the occurrence of grating lobes. Here, as shown in Fig. 3(d), periodicity of unit cell (p) does not affect the resonant frequency while influences the band reject frequency.

5. FABRICATION PROCEDURE

A prototype of 7×7 unit cells array is fabricated using ABS material with the help of 3-D printing or additive printing. The available software creality slicer is used for printing the prototype of size 175 mm $\times$ 175 mm. The proposed FSS is exported from CST microwave studio into .stl (stereographic) file. The .stl file is transferred to creality slicer printer, and this 3-D printer is set with some static and

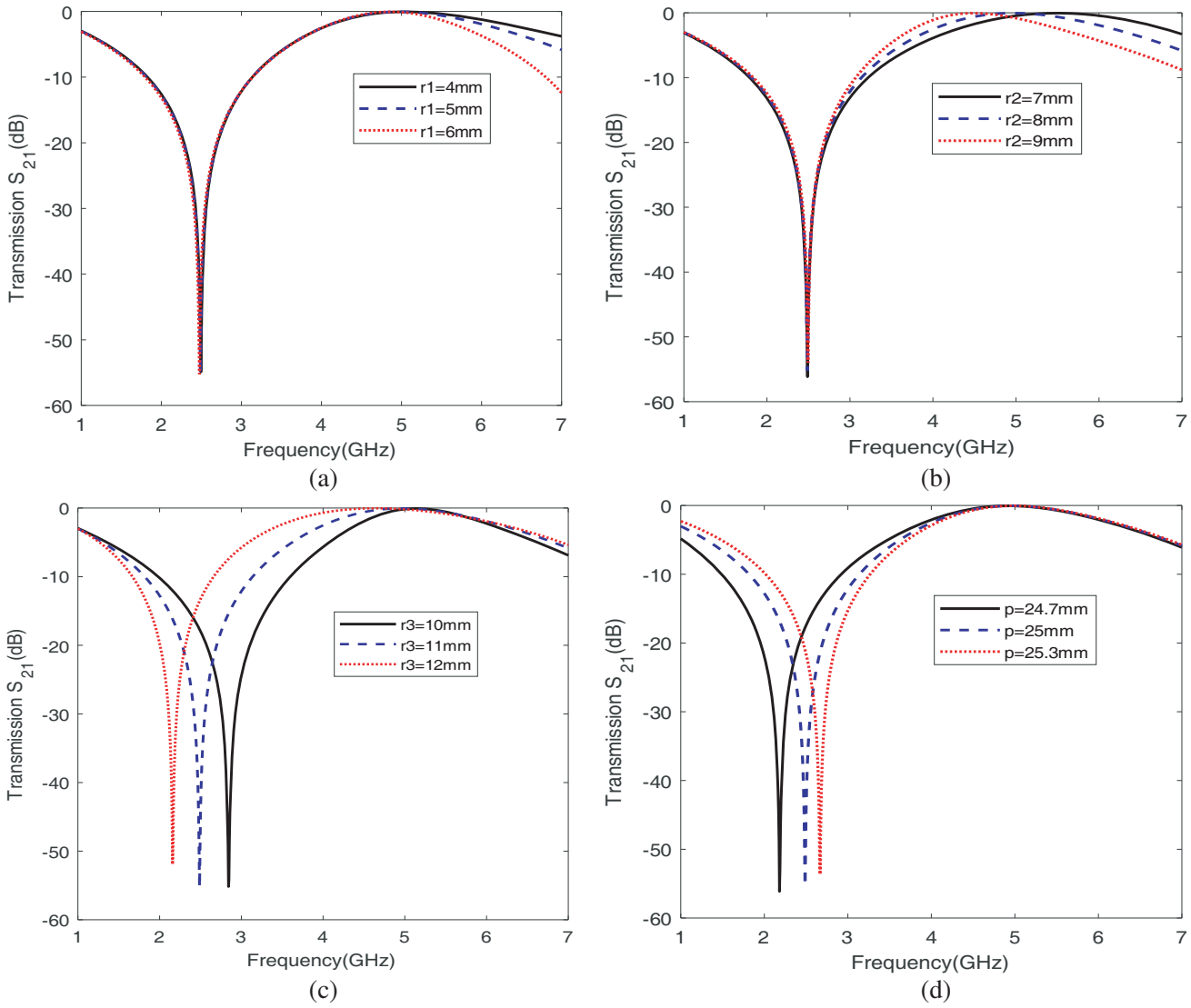

Figure 3. Showing effect of parameters (a) varying $r1$ and fixing other parameters (b) varying $r2$ and fixing other parameters (c) varying $r3$ and fixing other parameters (d) varying p and fixing other parameters.

variable parameters. The parameters are set for designing an FSS prototype on a 3-D printer include filament diameter of 175 mm, nozzle size of 0.4 mm, layer height of 0.3 mm, printing speed of 60 mm/s at bed temperature of 110°C and extrusion temperature of 240°C. The prototype is coated with copper conductive coating while leaving slots uncoated. The designed prototype is kept idle for 5–10 minutes and then tested further in free space measurement setup. The fabricated design can be seen in Fig. 4.

6. MEASUREMENT SETUP AND ANALYSIS OF RESULTS

To measure the frequency response of passive FSS design, a prototype is designed on an ABS material substrate with a thickness of 1.5 mm, dielectric constant $\xi_r = 2.8$, loss tangent of 0.0051, and grooved with thickness of 0.6 mm. The prototype can be viewed in Fig. 4. Two horn antennas covering the required frequency response are used as a transmitter and receiver during the measurement of the prototype and connected to VNA (vector network analyzer). The unobstructed measurement also called as free space measurement is set up for the proposed prototype as observed in Fig. 5(a). For

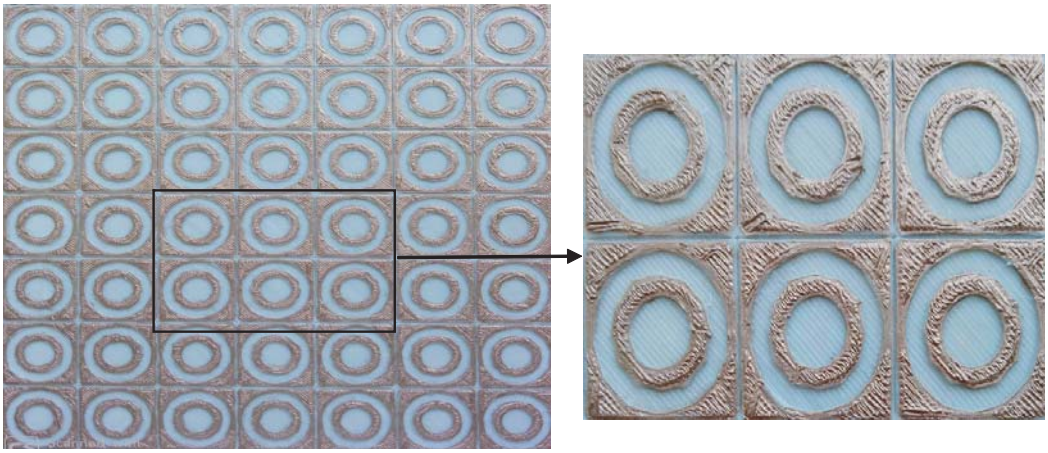

Figure 4. Fabricated prototype.

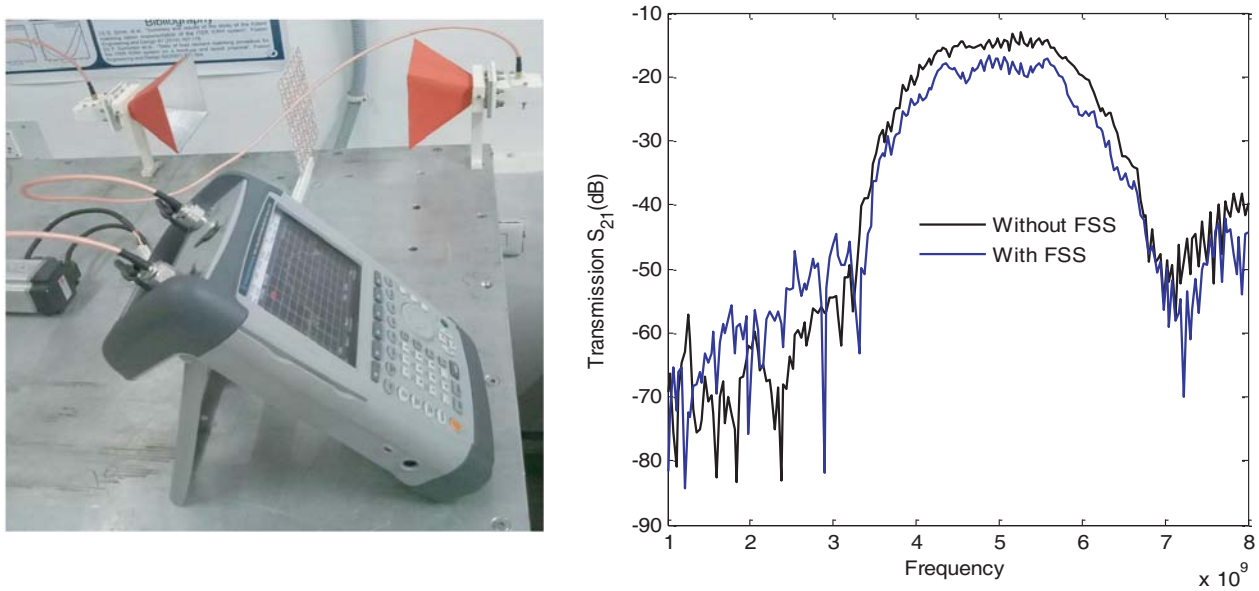

(a) (b)

Figure 5. (a) Measurement setup. (b) Experimental results with keeping FSS in between and without keeping FSS.

checking the accuracy of the experiment, the transmission coefficient is first measured without the FSS. Then the transmission coefficient is measured by keeping the FSS prototype between horn antennas. The results are shown in Fig. 5(b) without keeping the prototype and with keeping the prototype in between the antennas. It can be seen that there is approximately 15 dB coupling between the transmitting and receiving antennas. It is due to fabrication error since to make the whole process cost-effective, the transmitting and receiving horn antennas were also fabricated with 3-D printing material. The efficiency between the transmitting and receiving antennas can be found with the help of Friis transmission equation [20]:

$$\frac{P_r}{P_t} = \eta_t \eta_r D_t D_r \left(\frac{\lambda}{4\pi d}\right)^2 \tag{3}$$

or

$$\frac{P_r}{P_t} = G_t G_r \left(\frac{\lambda}{4\pi d}\right)^2 \tag{4}$$

where Pr and Pt are powers of receiving and transmitting antennas; Dt, Gt, Dr, and Gr are transmitting directivity, transmitting gain, receiving directivity, and receiving gain, respectively; λ is the wavelength of resonant frequency of designed FSS; d is the distance between transmitting and receiving antennas; η_t and η_r are transmitting and receiving antenna efficiencies, respectively. The measured experimental values are $P_t = 0\,\text{dBm}$, $P_r = -15.52\,\text{dB}$, $G = 15\,\text{dB}$, $d = 33\,\text{cm}$. The efficiency can be calculated using Equation (3), approximately as 61%. It can be said that due to the coupling between the two antennas, only 61% of transmitted power will be received by the receiver horn antenna. As seen in Fig. 5(b), experimental results are almost similar to simulated ones except that the band reject frequency is shifted at 2.85 GHz from 2.5 GHz.

The proposed work has been compared with previously reported FSS works as seen in Table 1. The proposed design is single layered unlike [22] and cost effective as compared with other works [21–24]. Ref. [25] is also cost effective and fabricated using 3-D printing, but due to less thickness of substrate material, there will be mutual coupling between the substrate layers which is compensated by our work. The proposed work mainly focuses on the reduction of cost and complexity in designing the prototype. This aim has been achieved as compared with previously designed FSS observed from Table 1.

Table 1. Comparison of proposed designed FSS with other previously designed FSSs.

	[21]	[22]	[23]	[24]	[25]	Proposed Design
Unit cell (mm)	6.7×6.7	12.6×12.6	9×9	42.51×42.51	16×16	25×25
Resonant Frequency (GHz)	3.96, 9 (dual band)	4	10.69, 26.5 (dual band)	3	1.05	5
Substrate Material	Rogers RO4003	RF-35	Arlon AD 320	Teflon	PLA	ABS
Fabrication Method	PCB technique	PCB technique	PCB technique	PCB technique	3-D printing	3-D printing
Substrate thickness (mm)	0.5	1.525	0.762	10	0.2	1.5
Number of conductive layers	1	3	1	1	2	1
Cost-effective	No	No	No	No	Yes	Yes

7. CONCLUSION

This paper deals with a 3-D printed frequency selective surface for harmonic radar applications. The proposed circular ring FSS is designed for 5 GHz resonant frequency. In order to make whole fabrication and measurement process cost-effective and easier for mass production, the horn antennas are also printed with ABS 3-D printing material. The simulated results suggest good angular stability of the proposed design at different incident angles. From transmission parameter (S_{21}), it is observed that metallic ring affects the resonant bandpass frequency while outer slot ring affects the band reject frequency. The periodicity of unit cell also affects the band reject frequency that is increased with increase in periodicity and vice versa. The prototype is validated with the experimental results to show good agreement with the measured results. Since the 3-D printing plastic material is easily available and fabrication process much easier than other fabrication techniques, this process can be used for a variety of future applications.

REFERENCES

1. Munk, B. A., *Frequency Selective Surfaces: Theory and Design*, John Wiley & Sons, 2005.
2. Reed, J. A. and D. M. Byrne, "Frequency-selective surfaces with multiple apertures within a periodic cell," *JOSA A*, Vol. 15, 660–668, Mar. 1998.
3. Sievenpiper, D. F., "High-impedance electromagnetic surfaces," 1998.
4. Ott, R. H., R. G. Kouyoumjian, and L. Peters, "Scattering by a two-dimensional periodic array of narrow plates," *Radio Science*, Vol. 2, 1347–1359, Nov. 1967.
5. Ebrahimi, A., S. Nirantar, W. Withayachumnankul, M. Bhaskaran, S. Sriram, S. F. Al-Sarawi, and D. Abbott, "Second-order terahertz bandpass frequency selective surface with miniaturized elements," *IEEE Transactions on Terahertz Science and Technology*, Vol. 5, 761–769, Jul. 2015.
6. Cong, L., X. Cao, and T. Song, "Ultra-wideband RCS reduction and gain enhancement of aperture-coupled antenna based on hybrid-FSS," *Radioengineering*, Vol. 26, 1041, Dec. 2017.
7. Zhang, W., J. Y. Li, and J. Xie, "A broadband linear-to-circular transmission polarizer based on right-angled frequency selective surfaces," *International Journal of Antennas and Propagation*, 2017.
8. Chakravarty, S., R. Mittra, and N. R. Williams, "On the application of the microgenetic algorithm to the design of broad-band microwave absorbers comprising frequency-selective surfaces embedded in multilayered dielectric media," *IEEE Transactions on Microwave Theory and Techniques*, Vol. 49, 1050–1059, Jun. 2001.
9. Parker, E. A., S. Massey, M. Shelley, and R. Pearson, "Application of FSS structures to selectively control the propagation of signals into and out of buildings Annex 5: Survey of active FSS," *ERA Technology, Tech. Rep. Ofcom AY4464A Project*, 2004.
10. Jain, A., R. P. Yadav, and S. Kumar, "Design and development of high power variable dual-directional radio frequency coupler," *IET Microwaves, Antennas & Propagation*, Vol. 13, 2544–2550, Aug. 2019.
11. Jain, A., R. P. Yadav, and S. Kumar, "Design and development of resonant loop antenna for mock-up ion cyclotron resonance frequency system of tokamak," *IET Microwaves, Antennas & Propagation*, Vol. 13, 976–981, 2019.
12. Jain, A., R. P. Yadav, and S. V. Kulkarni, "Design and development of 2 kW, 3 dB hybrid coupler for the prototype ion cyclotron resonance frequency (ICRF) system," *International Journal of Microwave and Wireless Technologies*, Vol. 11, 1–6, Feb. 2019.
13. Abadi, S. M. A. M. H., M. Li, and N. Behdad, "Harmonic-suppressed miniaturized-element frequency selective surfaces with higher order bandpass responses," *IEEE Transactions on Antennas and Propagation*, Vol. 62, No. 5, 2562–2571, 2014.
14. Chieh, J. C. S., B. Dick, S. Loui, and J. D. Rockway, "Development of a Ku-band corrugated conical horn using 3-D print technology," *IEEE Antennas and Wireless Propagation Letters*, Vol. 13, 201–204, Jan. 2014.
15. Kronberger, R. and P. Soboll, "3D-printed frequency selective surfaces for microwave absorbers," *IEEE International Symposium on Antennas and Propagation (ISAP)*, 178–179, Oct. 2016.
16. O'Neal, M. E., D. A. Landis, E. Rothwell, L. Kempel, and D. Reinhard, "Tracking insects with harmonic radar: a case study," *American Entomologist*, Vol. 50, 212–218, Oct. 2004.
17. Moore, J. D., "Acrylonitrile-butadiene-styrene (ABS)-a review," *Composites*, Vol. 4, 118–130, May 1973.
18. Liu, N., X. Sheng, C. Zhang, and D. Guo, "Design of frequency selective surface structure with high angular stability for radome application," *IEEE Antennas and Wireless Propagation Letters*, Vol. 17, 138–141, Nov. 2017.
19. Samaddar, P., S. De, S. Sarkar, S. Biswas, D. C. Sarkar, and P. P. Sarkar, "Study on dual wide band frequency selective surface for different incident angles," *Int. J. Soft Comput. Eng*, Vol. 2, 340–342, Jan. 2013.
20. Balanis, C. A., *Antenna Theory: Analysis and Design*, John Wiley & Sons, 2016.

21. Huang, F. C., C. N. Chiu, T. L. Wu, and Y. P. Chiou, "A circular-ring miniaturized-element metasurface with many good features for frequency selective shielding applications," *IEEE Transactions on Electromagnetic Compatibility*, Vol. 57, 365–374, Jan. 2015.
22. Behdad N., M. Al-Joumayly, and M. Salehi, "A low-profile third-order bandpass frequency selective surface," *IEEE Transactions on Antennas and Propagation*, Vol. 57, 460–466, Mar. 2009.
23. Bharti, G., K. R. Jha, G. Singh, G., and R. Jyoti, "Angular stable, dual-polarized and multiband modified circular ring frequency selective surface," *Frequenz*, Vol. 69, 199–206, May 2015.
24. Bharti, G., K. R. Jha, G. Singh, and R. Jyoti, "Design of angular and polarization stable modified circular ring frequency selective surface for satellite communication system," *International Journal of Microwave and Wireless Technologies*, Vol. 8, 899–907, Sep. 2016.
25. Ghosh, S. and S. Lim, "A miniaturized bandpass frequency selective surface exploiting 3D printing technique," *IEEE Antennas and Wireless Propagation Letters*, May 2019.